Mine Water and the Environment (2020) 39:808–822
https://doi.org/10.1007/s10230-020-00716-4

TECHNICAL ARTICLE

Groundwater Hydrogeochemical Mechanisms and the Connectivity of Multilayer Aquifers in a Coal Mining Region

Zhongyuan Yang[1] · Pinghua Huang[1,2] · Fengfan Ding[1]

Received: 15 December 2019 / Accepted: 17 September 2020 / Published online: 10 October 2020

Abstract

Multiple runoff connections for groundwater supply and water quality evolution mechanisms were disclosed using hydrochemistry, multivariate statistics, stable hydrogen and oxygen isotopes, and inverse hydrogeochemical modeling in a multilayer groundwater system in a north China coal-mining district. Groundwater quality was mainly influenced by dissolution and weathering of carbonate, silicate, gypsum, halite, and fluorite, as well as cation exchange. Sulfate enrichment in the Carboniferous limestone aquifer may be due to pyrite oxidation, while gypsum dissolution and sewage contribute sulfate to the Quaternary alluvium. The Ordovician limestone groundwater is hydraulically connected to the other two aquifers. Incongruent dissolution of dolomite occurs when the Ordovician limestone water contacts the Carboniferous aquifer, while evaporation occurs when the Ordovician limestone water migrates upward through fractures to the Quaternary aquifer.

Keywords Groundwater quality · Multivariate statistics · Stable isotopes · Hydrogeochemical modeling · Water–rock interaction

Introduction

Groundwater is an important source of drinking water in the North China Plain in eastern China. However, most coal mines in the area are underground operations, and this groundwater threatens safe operation and production as well as sustainable development of the water resources (Li 2018). Groundwater systems are often composed of various aquifers with various degrees of hydraulic connections. The input, output, and hydrochemical environment of the groundwater system must change as a response to mining activities, which results in complicated hydrogeological conditions and frequent water bursts in the mines (Chen et al. 2017). Therefore, studying the hydraulic connections of the different aquifers and how the groundwater migrates can be important in preventing underground water disasters and assuring sustainable utilization of groundwater resources.

Many methods have been used to study the hydrochemical characteristics and evolution of an area's groundwater system, including the ion ratio coefficient method (Barzegar et al. 2018; Fu et al. 2018) isotopic tracer method (Ayadi et al. 2018; Fu et al. 2018; Qian et al. 2013; Wang et al. 2012), multivariate statistics (Belkhiri et al. 2010; Li et al. 2019), geochemical modeling (Belkhiri et al. 2010; Carucci et al. 2012; Mendoza et al. 2016), hydrochemical mixing calculations (Martinez et al. 2017), Gibbs and Piper graph (Fu et al. 2018; Sako et al. 2016), scatter diagram (Ibrahim et al. 2019; Wang et al. 2012), and MODFLOW (Szymkiewicz et al. 2018). Scholars have analyzed the relationship between the type of water inrush source and multi-layer water-filled aquifers by simple comparisons of hydrochemical types, standard component judgment, microelement and isotope tracing, geochemical simulation, and so on (Huang et al. 2018a, b; Li et al. 2013; Liu et al. 2017; Qi et al. 2019; Xu et al. 2018).

In the coalfield, the primary concern of the area is the mine water and the potential for inrush. To rapidly identify water sources of major water aquifers, Wen et al. (2020) proposed a support vector machine (SVM) model based

Electronic supplementary material The online version of this article (https://doi.org/10.1007/s10230-020-00716-4) contains supplementary material, which is available to authorized users.

✉ Pinghua Huang
hph2001@hpu.edu.cn

[1] School of Resources and Environment Engineering, Henan Polytechnic University, Jiaozuo 454000, China

[2] Collaborative Innovation Center of Coalbed Methane and Shale Gas for Central Plains Economic Region, Jiaozuo 454000, China

on particle swarm optimization (PSO) and RBF kernel parameter optimization. Zhang et al. (2019a, b) established a multiple logistic regression recognition model for mine water source. The overall recognition accuracy of the model reached 86.6%. Various methods such as water chemistry, isotope tracing, and multivariate statistics were used to investigate the hydrogeochemical processes and hydraulic connectivity of multi-aquifer regional groundwater systems.

Li et al. (2016a) used hydrochemical characteristics and hydrogen and oxygen isotopes to examine the connectivity of river water and shallow groundwater. The same group subsequently assessed the connectivity of two adjacent aquifers using chloride ions (Li et al. 2018). Qian et al. (2014) used the $\delta^{18}O$ and $\delta^{2}H$ content to demonstrate three different recharge sources of the Yinchuan Plain lakes and estimate the evaporation proportion of each lake. Bawoke et al. (2019) used hydrogeochemical and isotopic methods along with hierarchical cluster analysis (HCA) and principal component analysis (PCA) to evaluate the hydrogeochemical and isotopic signatures of the Andasa water. The risk assessment model of water inrush from the coal seam floor has also been successfully applied to floor water inrush risk assessment for all of the north China-type coal mines (Shi et al. 2019).

The Jiaozuo coal mining district has complicated hydrogeological conditions and serious mine water disasters. The extremely abundant karst water is due to an extensive outcrop of Cambrian and Ordovician carbonates with karst fractures in the Taihang Mountains areas north of the Jiaozuo district. These carbonates have strong water-bearing capacity and are a major groundwater supply for the region (Fig. 1, Jin 2002). Huang et al. (2012) concluded that the groundwater in a major inrush aquifer might be supplemented by groundwater from the Taihang Mountains. They then used a Piper-PCA-Fisher water inrush source discrimination model to identify the source of 13 water inrush samples in the Jiaozuo coal-mining district and recognized all samples correctly except one, an accuracy of 92.3% (Huang et al. 2018a, b). Chen et al. (2015a, b) established hydraulic connectivity among the Jiaozuo coal-mining district aquifers based on the structure of the coal mining area, hydrochemistry, and isotopic characteristics. He et al. (2019) discussed the evolutionary trend of karst groundwater in the Jiaozuo mining area. And by analyzing examples of floor water inrush in the Jiaozuo mining area, Qiao (2011) proposed the regularity of water yield and the probability of water inrush.

Researchers have focused on identifying water inrush sources and proving the hydraulic connection of aquifers by comparing aquifer water chemical characteristics, and qualitatively evaluating risk of floor water inrush, but have not focused on the aquifer recharge sources and hydrogeochemical processes. No quantitative interpretation on the evolution process when groundwater in the bottom aquifer flows upward into the mines has been reported yet.

Therefore, in this study, water samples were collected from aquifers in the Jiaozuo coal mining district. The area's meteorology, groundwater storage, recharge, discharge, hydrogeological, hydrochemical, and lithologic characteristics, groundwater hydrogeochemical processes, and hydraulic connectivity of the main aquifers in the Jiaozuo district were analyzed using the ion ratio relationship and multivariate statistical methods. Furthermore, the main sources of recharge and flow direction between aquifers were determined by isotopic tracing and Durov diagrams. Finally, the recharge relationship of the groundwater was determined.

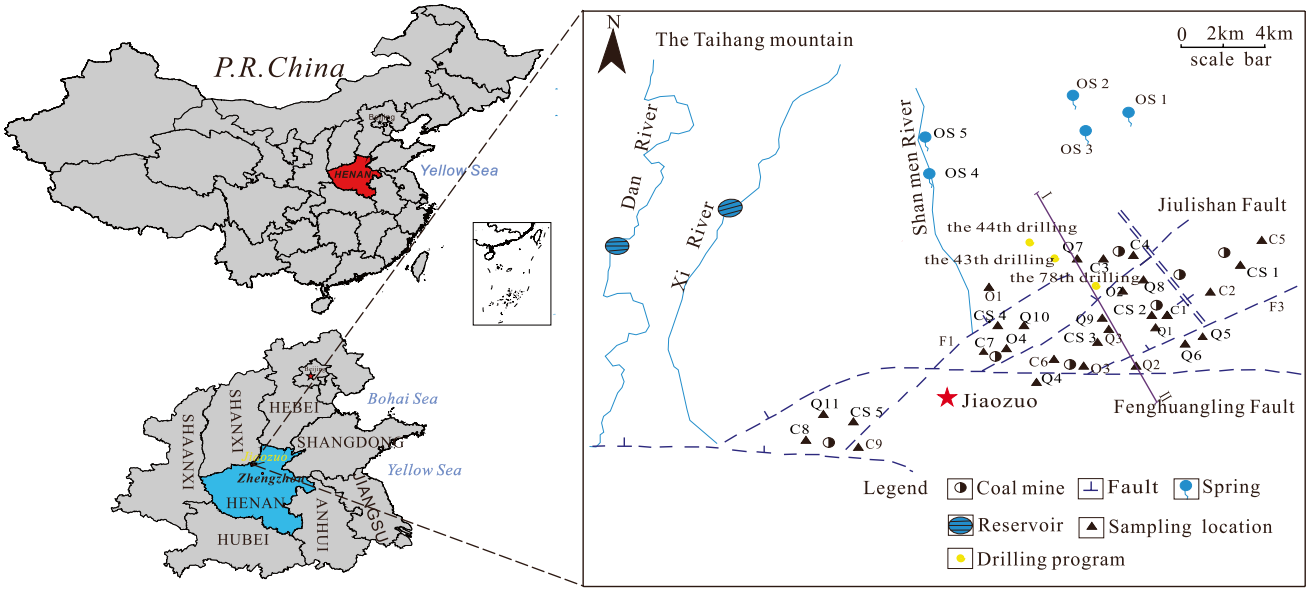

Fig. 1 Location map of the study area and sampling sites

Inverse geochemical modeling was used to explain the water-interaction processes. This study provides an effective research approach for future investigation of origin and migration of groundwater in mining areas.

Study Area

The north China coalfield in China refers to the coalfields south of the Yinshan structural belt, north of the eastern section of the Kunlun-Qinling structural belt, and east of the Helanshan structural belt to the Yellow Sea and Bohai Sea. It is mainly controlled by these three structural belts. The rock series is a set of Carboniferous-Permian strata, and the underlying Middle Ordovician thick carbonate strata. The Jiaozuo coalfield is an important component of the north-China coalfield and a famous inundated mine area (Fig. 1). Located in a piedmont diluvial fan at the southern foot of the Taihang Mountains, the coalfield is bordered by the Taihang Mountains to the north and the Yellow River to the south. The area has a temperate continental monsoon climate. The annual average precipitation declines gradually from the mountainous region in the north to the piedmont alluvial plain. The Jiulishan, Fenghualing, and Mafangquan Faults are the three major faults in the study area; these cut the entire coalfield into differently sized fault blocks. The horst and graben structure causes the region's complicated hydrogeological conditions. According to the lithology, thickness, aquiferous space, and depths of the formations, the major inrush aquifers in the study area are divided into four types (Fig. 2): (1) The porous Tertiary and Quaternary glutenites, which are mainly composed of Quaternary sandstone, clay, calcareous concretion, and bottom conglomerates. The supply sources of this water include atmospheric precipitation, irrigation, and infiltration from rivers and canals. (2) The coal-series sandstone aquifer is formed by alternating sandstone, siltstone, and shale strata. The osmotic coefficient is 0.1–0.3 m/d. The lower part is the $Second_1$ coal roof, which has a weak moisture content. Permeability is enhanced by water-conducting mining-induced fractures, which can influence coal exploitation to some extent. (3) The Carboniferous limestone aquifer is mainly composed of the Taiyuan Formation limestone and the stable L_8 and L_2 limestone karst aquifers. According to a pumping test, the osmotic coefficient is 1–3 m/d. The aquifer in the L_8 limestone is 2.72–11.32 m thick, is about 21 m from the $Second_1$ coal in the upper region, and is the direct water source for bottom water inrush during mining of this coal. (4) The Ordovician limestone aquifer is the sedimentation base of the coal measure strata and is composed of breccitic limestone, dolomitic limestone, and marlstone. The osmotic coefficient of the Ordovician limestone aquifer is 1–30 m/d. Aluminous mudstone in the upper region is the main aquiclude between the Carboniferous L_2 limestone and Ordovician aquifers, with an average thickness of 16.6 m. The Ordovician limestone aquifer has high water abundance, good connectivity, and a high pressure water head. It can supply water to the upper aquifers through water-conducting faults in the region.

The Taihang mountainous area north of Jiaozuo is a karst water replenishment area, with a large area of Cambrian-Ordovician carbonate rocks distributed on the surface. The surface and underground karst are well developed, and the mountainous area has abundant precipitation. The leakage of surface water along the river is also an important source of karst water supply in Jiaozuo. After replenishment in the north and west of Jiaozuo, the karst water flows from the north to the south and southeast to runoff in the piedmont discharge area. The karst water from the northern mountainous area moves through and is enriched by the strong water-conducting Fenghuangling, Jiulishan, and Zhucun faults, and forms a strong karst water runoff zone. The branch faults and small structures in the area are also well developed and interconnected, so that the karst water in the piedmont area has a uniform flow field and similar water level dynamics. Under natural conditions, karst water is discharged in clusters of springs on the southern side of Jiulian Mountain. Under the current mining conditions, artificial exploitation and mine drainage are the main forms of karst water drainage.

The piedmont and alluvial plains are relatively flat with well-developed surface vegetation, and the lithology of the aerated zone is mostly gravel, sand, and silty clay. The permeability is good, and atmospheric precipitation easily infiltrates and recharges the groundwater. In addition to infiltration of atmospheric precipitation, farmland irrigation water, and groundwater lateral runoff, leakage of mine water used to irrigate farmland in the western and eastern agricultural portions of the urban area, and the urban sewage used to irrigate farmland in the southern agricultural area of Jiaozuo are also important groundwater recharge methods. Dewatering, mine drainage, and groundwater evaporation are the main mechanisms of groundwater loss. In addition, groundwater is also discharged at springs and artesian wells.

Sampling and Methods

Water samples were mainly collected from public wells, hydraulic boreholes, a spring in the Taihang Mountains, and groundwater in the Jiaozuo coal-mining district (the positions of the samples are shown in Fig. 1). A total of 11 Quaternary groundwater samples, 5 coal-series groundwater samples, 9 Carboniferous limestone groundwater samples, 4 Ordovician limestone groundwater samples, and 5 Ordovician spring water samples were included in this study. All collected water samples were tested and analyzed in the field and laboratory. When sampling, samples were filtered by 0.45 μm film firstly in field. Bottles were

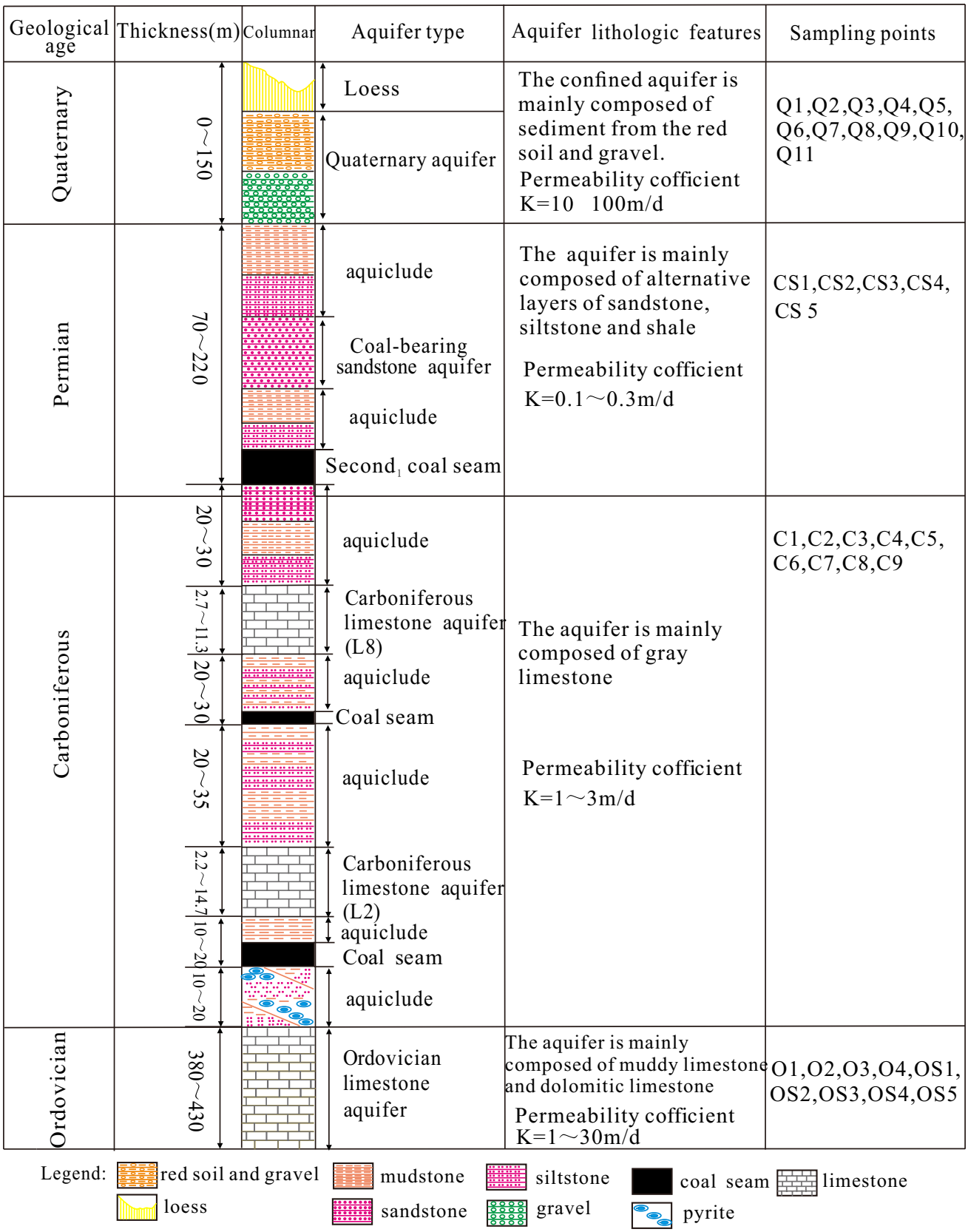

Fig. 2 Hydrogeology of the Jiaozuo coal-mining district

rinsed by water samples for three times before sampling. After sampling, pH, temperature (T), total dissolved solids (TDS), conductivity, acidity, and alkalinity were measured by portable equipment in the field. In the laboratory, pure HNO_3 was added to one bottle until a pH < 2 was reached; this was used for cation analysis by ICP-AES at the Resources and Environmental Experimental Center of Henan Polytechnic University. The other bottle was used for anion analysis using an ion chromatograph in the same laboratory.

In this study, multivariate statistical analysis, stable isotope and hydrogeochemical simulation were the main research methods. As an effective multivariate statistical analysis method, hierarchical cluster analysis (HCA) is mainly used for hydrochemical classification, aquifer connectivity, groundwater geochemical evolution, factors affecting groundwater pollution, and so on (Cortes et al. 2016; Pina et al. 2018; Qian et al. 2016; Sako et al. 2016; Voutsis et al. 2015; Wu et al. 2019). The basic principle of HCA is to make quantitative determination of genetic relationships among different samples using a mathematical method based on the concentrations of different components, and then divide samples into clusters based on such genetic relationships.

Factor analysis is a dimension reduction statistical method in multivariate statistics. It summarizes information reflected by multiple variables with a few representative variable combination factors and proposes the main influential factors of research objects. These factors can be used to explain complicated relationships among different hydrochemical components, recognize the main source of chemical components in water, and explain groundwater hydrochemistry genesis (Chen et al. 2015a, b; Lopes-Mazzetto et al. 2018; Wu et al. 2014; Zhang et al. 2019a, b).

Isotope and hydrochemical indexes are often used to solve hydrological problems. Hydrogen and oxygen isotopes are extensively used as a kind of tracer materials in hydrologic cycles (Jia et al. 2017; Peng et al. 2012). It is also used to recognize groundwater supply sources, supply conditions, groundwater mixing ratios, relations among different water bodies, and degree of evaporation (Huang et al. 2018a, b; Jin et al. 2018).

Inverse hydrogeochemical simulation is widely used in groundwater systems to determine reaction path and process from one point to another (Jia et al. 2017; Morán-Ramírez et al. 2016; Yang et al. 2018). Here, PHREEQC was used to simulate hydrogeochemical process along groundwater paths. PHREEQC is mainly used to calculate the saturation index (SI) of minerals (Table S-1). In addition, PHREEQC can be used to constructs a hydrogeochemical evolution model and calculate mineral conversion between two points along a groundwater flow path (Gastmans et al. 2010; Tizro et al. 2008; Yang et al. 2018).

Results and Discussion

General Chemical Properties

We analyzed water samples from the Quaternary, coal-series sandstone, Carboniferous limestone, and Ordovician limestone aquifers (Supplemental Table S-1). For the collected samples, EC = 0.25–1.28 mS/cm and the pH = 5.81–8.8, ranging from acid to alkaline. TDS = 317.4–1728.6 mg/L, which is a wide range. The major ions are: K^+ = 0.013–0.692 meq/L (small range), Na^+ = 0.087–12.243 meq/L, Mg^{2+} = 0.042–9.242 meq/L, Ca^{2+} = 0.215–7.27 meq/L, HCO_3^- = 3.041–11.233 meq/L (which fluctuates widely), SO_4^{2-} = 0.042–7.375 meq/L, Cl^- = 0.042–6.944 meq/L, and F^- = 0–0.342 meq/L (relatively stable).

There are three major hydrochemical types in the groundwater system: Ca-Na-HCO_3, Ca-Mg-HCO_3, and Na-HCO_3, and a few less common types: Na-Ca-HCO_3, Na-Mg-HCO_3, and Mg-Ca-HCO_3. The limestone aquifer is dominantly Ca-Mg-HCO_3 type water with low concentrations of TDS, EC, Na^+, K^+, SO_4^{2-}, and Cl^-. The coal-series sandstone aquifer mainly contains Na-HCO_3 type water. There are high concentrations of TDS, EC, Ca^{2+}, Mg^{2+}, SO_4^{2-}, and Cl^- in the Quaternary aquifer; hydrochemical types include Ca-Na-HCO_3, Ca-Mg-HCO_3, and Na-Mg-HCO_3. Ca^{2+}, Mg^{2+}, and Na^+ dominate the cations. The sulfate in the groundwater mainly comes from gypsum dissolution and sulfide oxidation, though the high concentrations of SO_4^{2-} (> 5.21 meq/L) and Cl^- in the Quaternary aquifer might be due to anthropogenic pollution (Zhang et al. 2010; Zhao 2017).

Changes of EC, TDS, and pH with increased sampling depth are shown in Supplemental Fig. S-1. EC and TDS show similar changes and are higher in the Quaternary aquifer than in the other aquifers, indicating mixed hydrochemistry. The TDS and EC at depths close to 150 and 300 m were elevated by sulfate generated by pyrite oxidation in the coal mine and resulting dissolved carbonates and silicates. The TDS and EC of the limestone water below 300 m are relatively low, indicating low salinity and a single hydrochemistry. The pH suddenly fluctuates in the depth range of 100–300 m and 500 m, revealing the complicated hydrochemical changes that are occurring in the relevant aquifers as a response to mining, faults, and other factors.

Table 1 XRD tests results of the cores samples from different aquifers

Aquifers	Minerals compositions calculated with XRD test	Potential hydrogeochemical progresses	Remarks
Quaternary aquifer	Mainly quartz with kaolinite	Minerals dissolution	Typical sandstone
Permain aquifer	Mainly quartz and kaolinite	Minerals dissolution and cations exchange	Typical sandstone and clay minerals
Carboniferous aquifer	Calcite dominates with less dolomite with pyrite	Carbonates system	Typical limestone
Ordovician aquifer	Calcite,dolomite,gypsum	Carbonates system	Typical limestone

Major Hydrogeochemical Processes

Mineral Phases: Dissolution and Precipitation

Based on the XRD test results (Table 1) of rock core from the main water inrush aquifers, the major minerals were dolomite, calcite, quartz, gypsum and clay minerals. The correlations of the dissolved components in groundwater with these minerals can be used to explain the source of solutes and chemical components of groundwater (Hussein et al. 2004). Relations among different ions were studied to further understand the geochemical aspects of the water quality changes.

Rock Weathering and Evaporation

Gibbs graphs (Gibbs 1970) can be used to explain the controlling mechanism of groundwater chemical components and lithological characteristics of aquifers and evaluate the influences of atmospheric precipitation, water–rock interaction, and evaporative deposition. It can be seen from Fig. S-2 that the hydrochemical components of the Ordovician, Carboniferous coal-series sandstone, and Quaternary aquifers in the mining area are mainly controlled by water–rock interaction. The high values in some Quaternary aquifer water sampling points indicates that this aquifer is also influenced by evaporation. Additionally, the ratio between $Cl^-/Cl^- + HCO_3^-$ and TDS is relatively low in most water sampling points, which reflects the limited influence of dissolution of carbonates on the hydrochemistry of the groundwater.

Cation exchange is also evident in Supplemental Fig. S-2. Despite the increase in $Na^+/Na^+ + Ca^{2+}$, the TDS remains basically constant, as 2 mol of Na^+ is exchanged with 1 mol of Ca^{2+}. Since the mass of 1 mol of Ca^{2+} is very similar to the mass of 2 mol of Na^+, the TDS remains basically the same.

Carbonate Minerals [$CaCO_3$, $CaMg(CO_3)_2$] and Gypsum ($CaSO_4$) -Ca^{2+},Mg^{2+},HCO_3^- and SO_4^{2-}

In Fig. 3a, two dissolution lines divide the graph into three regions. Two points of Carboniferous water are below $y = 2x$, which proves bicarbonate deficiency. Most of the Quaternary water and limestone water samples are close to or between these two lines, indicating that dissolution of calcite and dolomite is occurring, though exchange of Ca^{2+} might also be taking place. Coal-series sandstone water samples are all above $y = 4\times$ and bicarbonate ions are four times higher than Ca^{2+}. Therefore, dissolution of carbonate minerals might be accompanied with abundant cation exchange or weathering of silicate minerals. Most Quaternary water and limestone water samples (Fig. 3b) are on or close to the dolomite dissolution line.

Figure 3c provides evidence of gypsum in the four aquifers, with correlation coefficients close to 0.5 (Ca^{2+}, $R^2 = 0.6$; SO_4^{2-}, $R^2 = 0.4$). In a correlation diagram of $Ca^{2+} + Mg^{2+}$ and sulfate ions, $Ca^{2+} + Mg^{2+}/SO_4^{2-}$ is 1:1 if $Ca^{2+} + Mg^{2+}$and SO_4^{2-} in groundwater only come from gypsum dissolution. In Fig. 3d, most coal-series sandstone water samples are on the gypsum dissolution line, indicating this water is also strongly influenced by gypsum. In contrast, Quaternary and limestone water samples are far above the 1:1 line. The excess Ca^{2+} mainly comes from dissolution of carbonate minerals, while the SO_4^{2-} is mainly provided by gypsum dissolution.

If the HCO_3^-, SO_4^{2-}, Ca^{2+}, and Mg^{2+} in the deep groundwater are all from dissolution of sulfate and carbonate minerals, sampling points on the correlation map between $HCO_3^- + SO_4^{2-}$ and $Ca^{2+} + Mg^{2+}$ concentrations should fall along the 1:1 line (Liu et al. 2015). Most Quaternary water and limestone water points in Fig. 4d distribute along the line of $\gamma(HCO_3^- + SO_4^{2-})/\gamma(Ca^{2+} + Mg^{2+}) = 1{:}1$, but the coal-series sandstone water samples are above $y = x$, indicating that these cations are being removed by adsorption or dissolution of silicate, thus balancing residual anions. Quaternary sampling points Q1 and Q5 have slightly high SO_4^{2-} content ($SO_4^{2-} > 7.31$ meq/L). Due to the discharge of industrial and mining enterprises wastewater, the overall content of SO_4^{2-} ions in shallow groundwater in the study area is relatively high, exceeding the 5.21 meq/L standard limit.

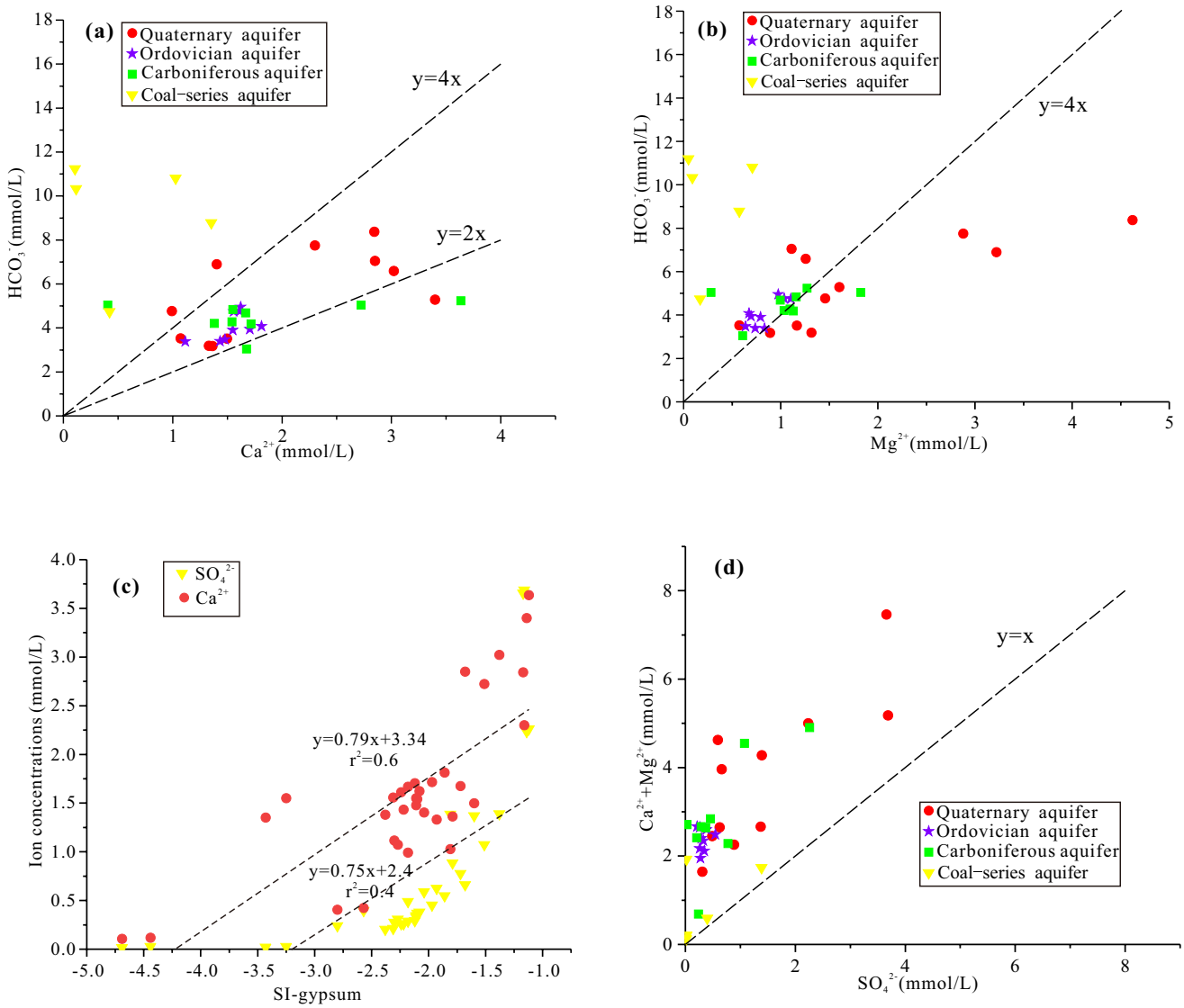

Fig. 3 Scatterplots displaying the ionic relationships Ca^{2+} vs HCO_3^- (**a**), Mg^{2+} vs. HCO_3^- (**b**), SI-gypsum vs. Ca^{2+} and SO_4^{2-} (**c**), $Ca^{2+}+Mg^{2+}$ vs. SO_4^{2-} (**d**)

Clay Minerals and Cation Exchange (NaX, CaX_2)

The relationship of Na^+ and Cl^- in groundwater is shown in Supplemental Fig. S-3a. Most limestone water sampling points are on $y=x$, indicating that the Na^+ in the limestone water likely comes from the leaching of halite. Nevertheless, Quaternary water samples and coal-series sandstone water samples are below $y=x$. This reflects that Na^+ is supplied by dissolution of sodium salt minerals or cation exchange in addition to leaching of halite; the Cl^- mainly come from halite dissolution. The Cl^- concentration at the Quaternary sampling point Q1 was 246.5 mg/L, which might be due to Cl^- pollution. In addition, the slope of $Na^+ + K^+$-Cl^- vs $Ca^{2+} + Mg^{2+}$-SO_4^{2-}-HCO_3^- is -1, which also can reflect cation exchange (Ahmed et al. 2013). The correlation coefficient between $Na^+ + K^+$-Cl^- and $Ca^{2+} + Mg^{2+}$-SO_4^{2-}-HCO_3^- in all sampling points of Jiaozuo coal-mining district reaches 0.93 (Fig. S-3b), indicating the extensive occurrence of cation exchange in the inrush aquifers.

According to the relationship between Ca^{2+}/Na^+ and Mg^{2+}/Na^+ at sampling points in the study area (Fig. 4b, c), the ratio of major ion concentrations (mole fraction) of most Quaternary and limestone water primarily indicate dissolution of silicate and carbonate minerals. Nevertheless, coal-series sandstone water is dominated by evaporation of salt and dissolution of silicate minerals.

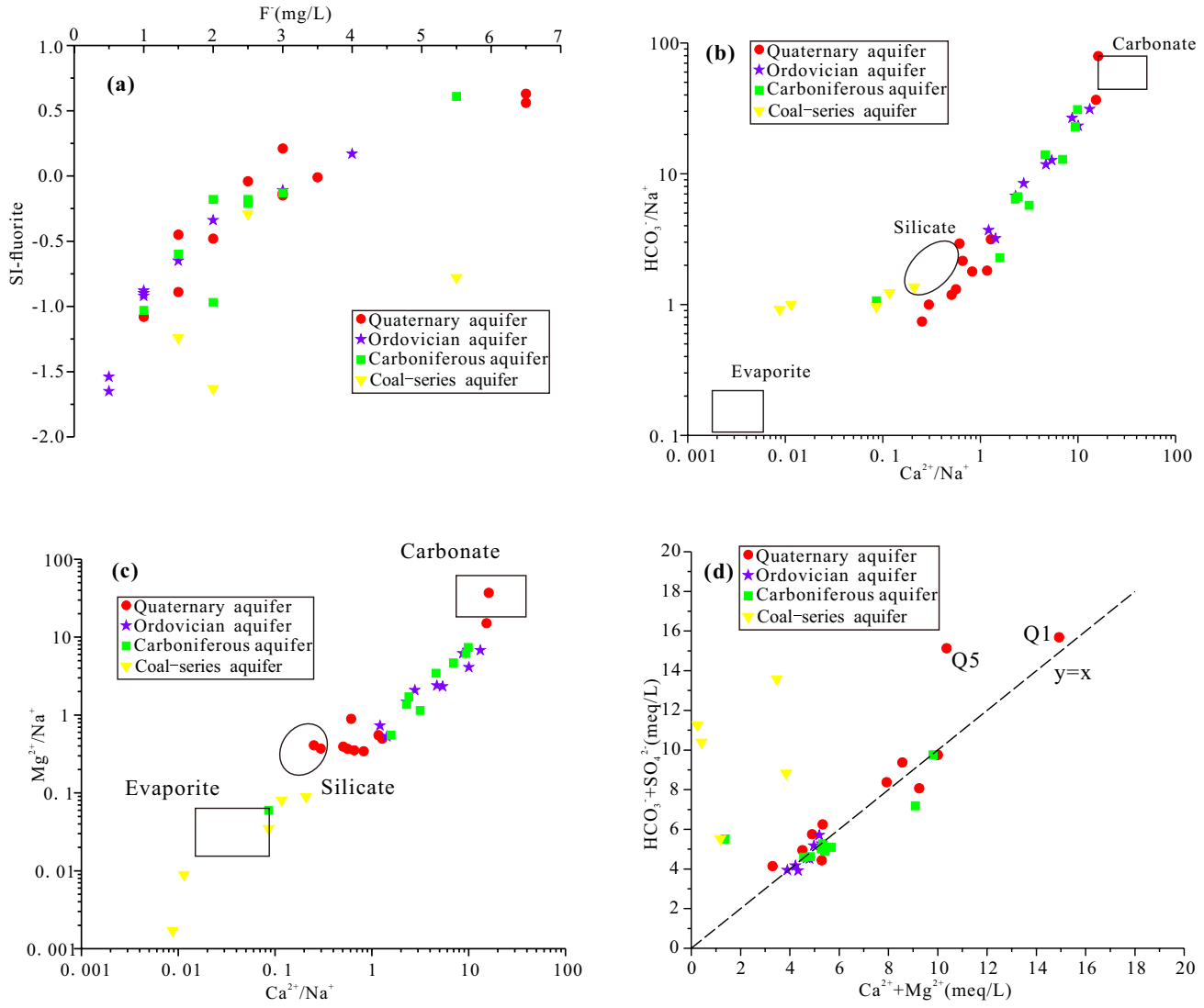

Fig. 4 Scatter diagrams showing the ionic relationships between SI-fluorite vs. F^-(**a**), Ca^{2+}/Na^+ vs. HCO_3^-/Na^+ (**b**), Ca^{2+}/Na^+ vs. Mg^{2+}/Na^+ (**c**), $Ca^{2+}+Mg^{2+}$ vs. $HCO_3^-+SO_4^{2-}$ (**d**)

Fluoride (CaF_2) Sources

F^- in the study area ranges between 0–6.5 mg/L, 2.43 mg/L in average. Dissolution of fluoride in groundwater is relatively small and it cannot dominate influences to hydrochemical components of groundwater. PHREEQC has calculated the SI of fluorite in the aquifer samples (Fig. 4a) and it less than 0 in most water samples, with a gradually decreasing slope.

Factor Analysis

In this study, K^+, Na^+, Ca^{2+}, Mg^{2+}, HCO_3^-, SO_4^{2-}, Cl^-, and F^- indicators were used as the initial factor analysis variables to indicate the hydrogeochemical processes that occur in the groundwater. The correlation matrix (Supplemental Table S-2) reveals correlations among ions in water samples from different aquifers. The correlation coefficient of K^+ with Na^+ is the highest (0.927) and its correlation coefficient with HCO_3^- is the second highest (0.834), which might be due to dissolution of bicarbonate. However, K^+ is negatively correlated with Ca^{2+} and Mg^{2+}, which might be caused by cation exchange. Na^+ is highly correlated with HCO_3^- and Cl^-, indicating dissolution of silicate and salt rock minerals. The high correlation between Mg^{2+} and Cl^- is the collaborative consequence of dissolution of salt rock and inverse cation exchange. Correlation between Mg^{2+} and SO_4^{2-} reflects dolomite dissolution by the acidity generated by pyrite oxidation. Correlation between Ca^{2+} and SO_4^{2-} implies dissolution of gypsum. The correlation coefficient between Ca^{2+}

and Mg^{2+} is 0.530, which discloses a carbonate system. However, there's a negative correlation between HCO_3^- and Ca^{2+} as a result of cation exchange or the precipitation of calcite at higher calcium ion concentrations.

Factor load is determined by principal component analysis (PCA). Two common actors (F1 and F2) are extracted and their cumulative contribution rate reached 81.40%. It is believed that F1 and F2 could reflect basic information of original data well. Factors are rotated by the maximum variance method and coefficients matrix of the species (Supplemental Table S-3) is gained, which can better explain the actual meaning of the factors.

The contribution rate of F1 is 49.51%. The loading scores of Ca^{2+}, Mg^{2+}, Cl^-, and SO_4^{2-} are relatively high (0.772–0.898) and are positively correlated with F1. It is speculated that F1 represents dissolution of carbonate, gypsum, halite, and fluorite (Table 1) as well as the relationship between sulfate ions and carbonate dissolution. The contribution rate of F2 is 31.88%. The loading scores of Na^+, K^+, and HCO_3^- are relatively high (0.899–0.971) and are positively correlated with F2. However, Ca^{2+} and Mg^{2+} are negatively correlated with F2, indicating cation exchange. Based on the mineral composition of the aquifers (Table 1) and Fig. 4b, c, it is speculated that F2 is related to weathering of silicate minerals (e.g. feldspar) and cation exchange.

Scores of different samples on these two common factors are shown in Fig. 5. Most Quaternary water samples have high F1 scores. The average SO_4^{2-} concentration of water samples Q1, Q2, Q4–Q6, Q11, C8, and C9 is 187 mg/L. Since there is no sulfide in the Quaternary aquifer (Table 1), the fact that samples Q2, Q4, Q6, and Q11 are enriched in sulfate in F1 is due to gypsum dissolution rather than sulfide oxidation. The SO_4^{2-} concentrations of Q1 and Q5 in F1 is above 351 mg/L, due to the discharge of industrial wastewater, acid mine drainage (Yu et al. 2012), and sulfate-containing sewage. C8 and C9 from Carboniferous limestone aquifer may might be due to the oxidation of pyrite.

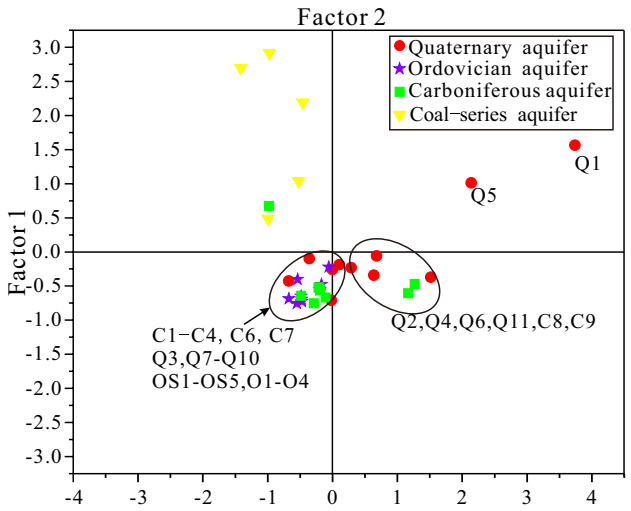

Fig. 5 Factor scoring diagram

The coal-series sandstone water samples have high F2 scores. On this basis, it is inferred that this water is affected by weathering of silicate minerals and cation exchange. Most Ordovician and Carboniferous limestone water samples have high F1 scores, reflecting dissolution of carbonate, gypsum, halite, and fluorite. Ordovician limestone water samples overlap with Carboniferous limestone water samples, which suggests possible mixing between Ordovician (OS1–OS5, O1–O4) and Carboniferous limestone water (C1–C4, C6, C7). Some Quaternary water samples (Q3, Q7–Q10) overlap with limestone water samples, which suggests possible mixing between Quaternary water and limestone water. To verify these assumption, HCA analyses, stable isotope analyses, and Durov diagrams were used to identify the groundwater sources connectivity and determine their flow direction.

Determination of Aquifer Connectivity and Groundwater Flow Direction

Hierarchical Cluster Analysis

Q-type clustering analysis is a statistical method that divides samples into several types based on similarity of variables (Xu et al. 2019; Zhang et al. 2014). The 34 water samples were analyzed for major discrimination indexes (Ca^{2+}, Mg^{2+}, Na^+, K^+, SO_4^{2-}, Cl^-, HCO_3^-, F^-). Data were normalized before Q-type clustering analysis of the hydrochemical composition data (Table S-1), and distance was calculated by the Ward and square Euclidean distance methods. Four clusters were determined (Fig. 6). In Cluster 1, both Quaternary water samples (Q3, Q7–Q10), and Carboniferous and Ordovician water samples (C1–C4, C6, C7, OS1–OS5, O1–O4) have similar Ca-Mg-HCO_3 hydrochemical characteristics, which is different to C5 and CS3 that contain Na-HCO_3. Coal-series sandstone water samples (Cluster 2) are significantly different from the water in other aquifers, with Na-HCO_3 type water, suggesting that the coal-series sandstone aquifer is relatively isolated, and that no hydraulic connection exists between it and the underlying Carboniferous and Ordovician limestone aquifers under natural conditions. Samples Q1 and Q5 in Cluster 3 are Na-Mg-HCO_3-SO_4 type, with SO_4^{2-} concentrations above 350 mg/L, due to surface contamination. The samples of Cluster 4 also show Ca-Mg-HCO_3 hydrochemical characteristics, but the average of ion concentrations is higher in Cluster 1.

Durov Diagrams

Durov diagrams can disclose connections between aquifers and the geochemical evolution of groundwater (Li et al.

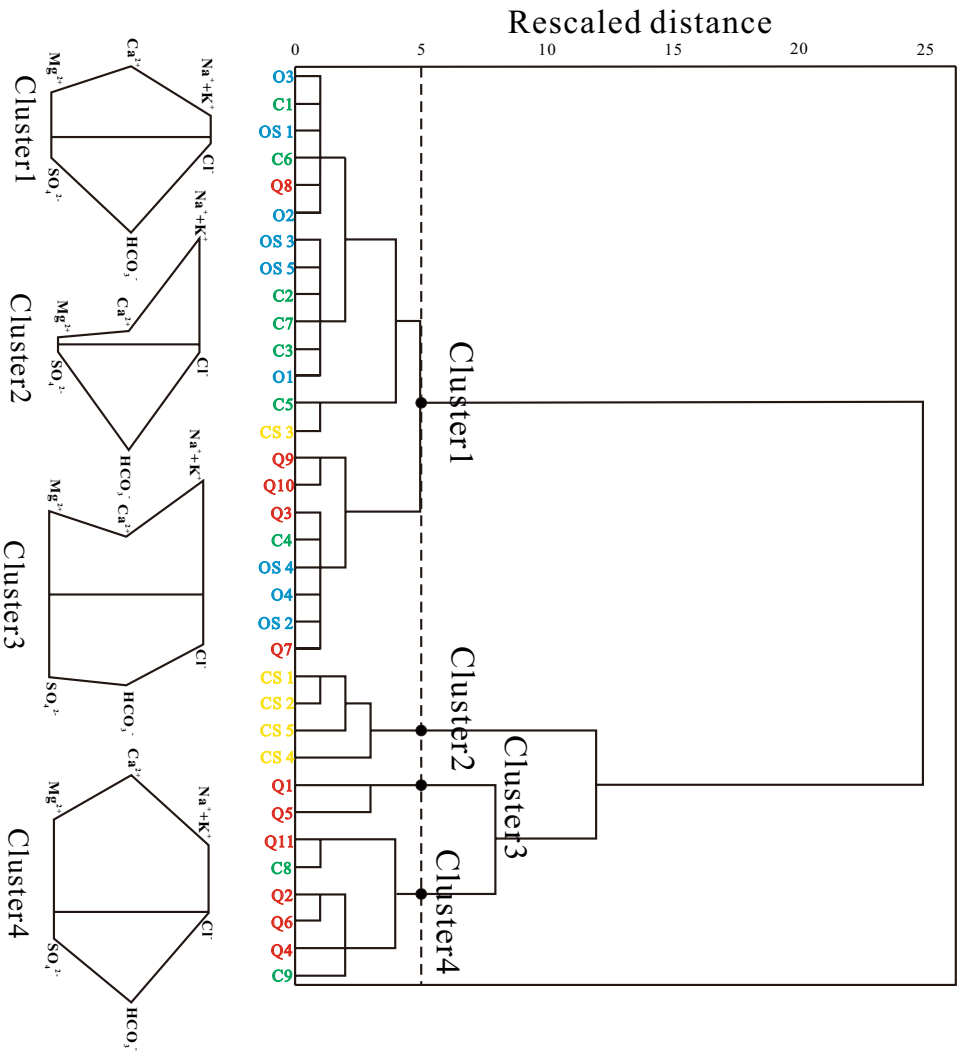

Fig. 6 Clustering analysis of water samples

2016b; Xu et al. 2019). It can be seen from Supplemental Fig. S-4 that the limestone water samples are in region 7, due to the low salinity of the limestone water, and is similar to the modern infiltration water (Makni et al. 2013). Carboniferous and Ordovician water samples are similar, indicating that there might be hydraulic connections. The deeper limestone water dominated by Ca-Mg-HCO_3 enters the Quaternary water system, which is mainly a mixture of Ca-Mg-Na-HCO_3, Ca-Na-Mg-HCO_3, and Na-Mg-Ca-HCO_3 types in region 5, and TDS increases accordingly. The water samples from the coal-bearing sandstone aquifer are distributed independently in region 9, suggesting no contact with other aquifers.

Isotope Analyses

Figure 7a shows that the meteoric water line is $\delta D = 8\delta^{18}O + 10$. The local meteoric water line (LMWL): $\delta D = 6.75\delta^{18}O - 2.74$ of Zhengzhou City, Henan Province is also shown. There are few Ordovician and Carboniferous limestone water samples close to the local precipitation line, showing the limited influence of rainfall infiltration. The Quaternary water samples in circle A are located at the lower right of the local meteoric water line, indicating that the hydrogen and oxygen isotopes were enriched by evaporation. In Fig. 7b, chlorine ions gradually increase along the groundwater flow path, and the $\delta^{18}O$ value also gradually moves to the right. The Quaternary water samples (Q1, Q7, Q10) are located at the far right, again indicating that the Quaternary aquifer has been affected by evaporation.

Most points are close to the local groundwater line (LGWL) in basic symmetric distribution, indicating the consistent source of these points. The $\delta^{18}O$ in the frame of Fig. 7b fluctuates within a small range (−9.26‰–−8.20‰). However, Cl^- begins to enrich vertically along the y-axis, which further reflects the flow direction of groundwater. Because the water abundance of the Carboniferous limestone aquifer in the Jiaozuo mining area is weak, and has been affected for a long time by mine dewatering, the flow of the Carboniferous limestone water was not considered.

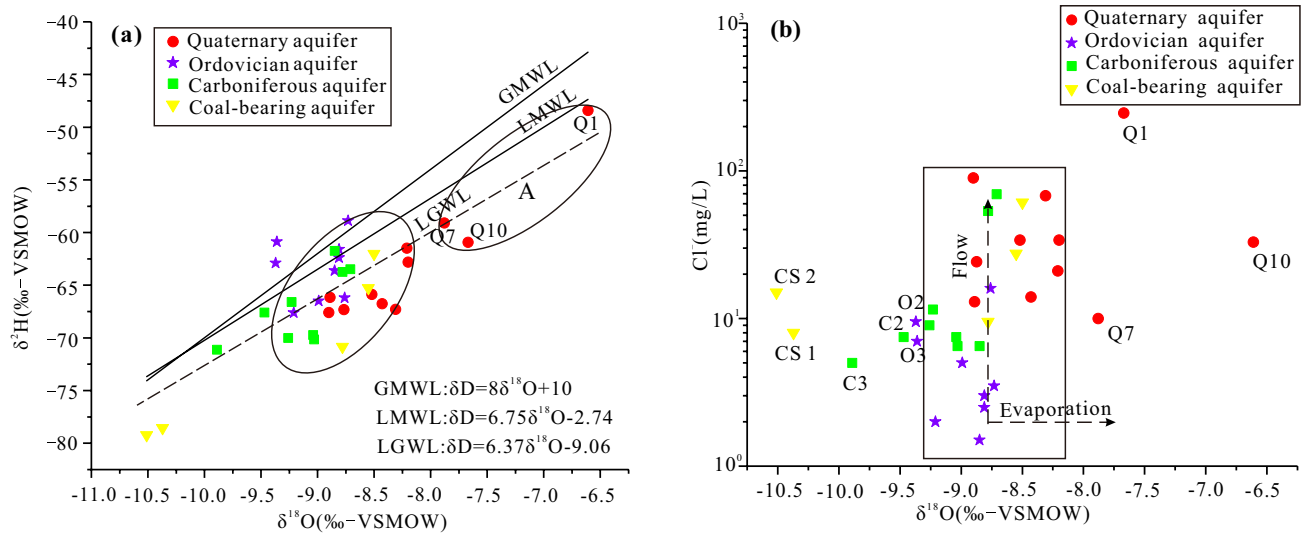

Fig. 7 Relationship between: **a** $\delta^{18}O$ vs. $\delta^{2}H$ from water samples; **b** $\delta^{18}O$ vs. Cl^- content

Quaternary and Carboniferous limestone water samples Q3, Q8, Q9, C1, C4, C6, and C7 are all distributed near large faults (Fig. S-5) and appear to show the influence of Ordovician limestone water (OS1–OS5, O1, O4). Combined with the factor analysis, HCA results, and Durov diagrams, it is confirmed that these seven samples reflect mixing.

Inverse Geochemical Modeling

Combined with the factor analysis and cluster analysis results, it is speculated that water samples Q3, Q7–Q10 C1–C4, C6, C7, OS1–OS5, and O1–O4 may be mixed through the surrounding fault structure, producing their close chemical properties (cluster 1). After that, the Durov diagram and isotope tracer technique verify that the three water samples (Q3, Q8, Q9) from the Quaternary aquifer and four water samples (C1, C4, C6, C7) from the Carboniferous limestone aquifer were influenced by the Ordovician limestone aquifer (OS1–OS5, O1, O4). Thus, two groundwater hydraulic connections were established. Inverse geochemical modeling was used to interpret the hydrochemical evolution and multi-component chemical reactions resulting from the aquifers' connections. The average value of the water samples of the Ordovician limestone was used to represent initial point, and the average value of the water samples of the Quaternary aquifer and Carboniferous aquifer represent the final point (Table 2).

Possible Mineral Phases

In this study, we restricted our attention to the major mineral phases for inverse geochemical modeling, According to the XRD test results, groundwater composition characteristics, and hydrogeochemical processes, calcite, dolomite, gypsum, halite, and fluorite were chosen as the possible mineral phases. Since clay minerals are important substances in aquifers, cation exchange also had to be assessed. Pyrite was not considered due to its low concentrations. Because the shallow groundwater is in an open system, it is affected by evaporation. CO_2 and H_2O also had to be accounted for. The mineral phases and corresponding reactions are shown in Supplemental Table S-4.

deep Limestone Aquifer Connections

The mean value of the Ordovician and Carboniferous limestone aquifer water samples were chosen for geochemical modeling using calcite, dolomite, fluorite, gypsum, and

Table 2 Mean parameter values of the three major aquifers

	pH	T	Na^+	K^+	Ca^{2+}	Mg^{2+}	HCO_3^-	SO_4^{2-}	Cl^-	F^-
Q ($n=3$)	7.98	19.57	35.8	4.23	50.93	31.53	233.33	79.5	18.67	2.17
C ($n=4$)	7.4	21.4	9.2	0.75	66.08	23.35	255.48	37	7.38	2.38
O ($n=7$)	7.33	16.04	8.97	1.58	60.86	18.77	234.6	31	4.79	1.07

All values are in mg/L except pH and T (℃)

Q Quaternary aquifer, *C* Carboniferous limestone aquifer, *O* Ordovician limestone aquifer

halite as the mineral phases, along with CO_2 and cation exchange. The SI of calcite and dolomite is less than 0 at the starting point and exceeds 0 at the end point, reflecting dissolution. The SI of gypsum, fluorite, and halite were also less than 0 and increased slightly, indicating the strong dissolution of these minerals.

Table 3 shows the process of water–rock interactions when the Carboniferous and Ordovician limestone aquifers are connected, and the perfect connection between the two limestone aquifers; the fraction of initial water is 1 ± 0.035. The incongruent dissolution of dolomite dominates during upward migration of the groundwater, though gypsum, halite, and fluorite all dissolve as well. However, calcite precipitates, proving the incongruent dissolution of dolomite. CO_2 was consumed by dolomite dissolution. Cation exchange mainly releases Ca^{2+} and adsorbs Na^+. Dissolution of dolomite and gypsum exceeds calcite precipitation, resulting in an increase of Ca^{2+}, Mg^{2+}, and SO_4^{2-}. PHREEQC indicates that the Carboniferous limestone receives water from the lower Ordovician limestone, which increases the risk of water inrush at the mine.

The Ordovician and Carboniferous limestone water samples have a similar water chemistry, and the lithology is dominated by calcite and dolomite. Due to the depth of the carbonate system, dissolution was all < 1 mmol/L. Water rock interaction was assumed to be the principal mechanism of the evolution of water chemistry. The dissolved constituents in the Carboniferous limestone water primarily come from the incongruent dissolution of dolomite, followed by a small amount of evaporite mineral dissolution (e.g. halite and gypsum) and fluorite as well as sodium adsorption.

Shallow And Deep Groundwater Connections

As already described, Ordovician limestone water migrates upward in the study area. To further verify the hydraulic connection between shallow and deep aquifers, the mean chemical parameter values of two aquifers were used to represent initial and final waters along the groundwater flow direction (Table 2). PHREEQC only finds two models with an uncertainty degree of 0.05. Table 4 indicates that the Ordovician aquifer with its high head pressure is the Quaternary aquifer's main water source. Evaporation in the

Table 3 Result for the inverse geochemical modeling among limestone aquifers

Aquifer and Phases	Formula	Fractions and mole transfer (mol/L)		Indications
		O-C (final)		
O		1	1	Concentrated
C		1	1	–
Calcite	$CaCO_3$	−1.911e−04	−1.911e−04	Precipitation
Dolomite	$CaMg(CO_3)_2$	1.842e−04	1.842e−04	Dissolution
Gypsum	$CaSO_4{\cdot}2H_2O$	6.685e−05	6.685e−05	Dissolution
Halite	NaCl	7.297e−05	7.297e−05	Dissolution
Fluorite	CaF_2	3.432e−05	3.432e−05	Dissolution
CO_2 (g)	CO_2 (g)	9.326e−05	–	CO_2 consumed
NaX	NaX	−6.354e−05	−6.354e−05	Ion exchange
CaX_2	CaX_2	3.177e−05	3.177e−05	Ion exchange

Table 4 Result for the inverse geochemical modeling between shallow and deep aquifers

Aquifer and phases	Formula	Fractions and mole transfer (mol/L)		Indications
		O-Q (final)		
O		3.734	3.894	Concentrated
Q		1	1	–
Calcite	$CaCO_3$	−2.284e−03	−2.361e−03	Precipitation
Dolomite	$CaMg(CO_3)_2$	−1.571e−03	−1.691e−03	Precipitation
Gypsum	$CaSO_4{\cdot}2H_2O$	−3.711e−04	−4.038e−04	Precipitation
Halite	NaCl	2.246e−05	–	Dissolution
Fluorite	CaF_2	−4.828e−05	−5.279e−05	Precipitation
CO_2 (g)	CO_2 (g)	−6.592e−03	−6.953e−03	CO_2 released
H_2O (g)	H_2O (g)	−1.518e+02	−1.607e+02	H_2O released

Quaternary aquifer results in a higher hydrogen and oxygen isotope value than in the Ordovician limestone water. The associated water loss is ≈151.8–160.7 mol/L. Calcite, dolomite, fluorite and gypsum are all precipitating, while halite is dissolving. The amount of minerals lost to precipitation (4.30 mmol/L) exceeds the amount of dissolved minerals (0.022 mmol/L), leading to CO_2 being released.

The two major hydraulic connections among aquifers form the groundwater "circulation" in Supplemental Fig. S-5. The connectivity of the complex multi-layer groundwater water system can be employed to predict water inrush sources and groundwater resource protection in other mining areas, since most of the north China coal mines have similar hydrogeological structures.

Conclusions

In this study, hydrochemistry, multivariate statistics, isotope analysis, and inverse geochemical modeling were used to disclose the groundwater evolution processes and aquifer connectivity in the Jiaozuo mining area. The main conclusions are:

1. The geochemistry of the Quaternary, Ordovician, and Carboniferous limestone aquifers is mainly influenced by dissolution of calcite, dolomite, gypsum, halite, and fluorite, while the coal-series sandstone aquifers mainly show the effect of silicate mineral dissolution and ion exchange. In addition, the Quaternary aquifer is influenced by evaporation and sulfate pollution from sewage. Pyrite oxidation adds to the enrichment of sulfate ion in the Carboniferous limestone aquifer.
2. Factor analysis, HCA, Durov diagrams, and stable isotope analyses show that three of the water samples from the Quaternary aquifer and the four from the Carboniferous limestone aquifer were supplied by upward vertical migration of Ordovician limestone groundwater via fractures.
3. The inverse geochemical modeling showed that two hydrogeochemical evolution paths were applicable. During the migration of Ordovician limestone water to the Carboniferous aquifer, incongruent dolomite dissolution dominates, followed by ion exchange, and dissolution of gypsum, fluorite, and halite. Evaporation was confirmed as Ordovician limestone water flows upward to the Quaternary aquifer through fracture structures, encountering more atmosphere closer to the surface, resulting in mineral precipitation.
4. Ordovician limestone water with strong water abundance is the main water source and supplies water to the shallow aquifer through water-conducing faults. As mining migrates into deeper strata, karst water below the coal series has a high water head and water yield. Karst water has become the most threatening potential problem in the area. The fault zones and cracked intensive belts at two sides are main channels for water. Preventive measures must be adopted to prevent water inrush accidents in coal mines.

Acknowledgements This work was financially supported by the National Natural Science Foundation of China (Grant 41672240), Science and Technology Key Research Project of the Education Department of Henan, China (13A170313 & 14A510022), China Postdoctoral Science Foundation (2017M612395), Innovation Scientists and Technicians Troop Construction Projects of Henan Province (Grant CXTD2016053), Henan Province's Technological Innovation Team of Colleges and Universities (Grant 15IRTSTHN027), Fundamental Research Funds for the Universities of Henan Province (NSFRF1611), Scientists and Technicians Projects of Henan Province (Grant 182107000019).

References

Ahmed MA, Samie SG, Badawy HA (2013) Factors controlling mechanisms of groundwater salinization and hydrogeochemical processes in the Quaternary aquifer of the Eastern Nile Delta. Egypt Environ Earth Sci 68(2):369–394

Ayadi R, Trabelsi R, Zouari K, Saibi H, Itoi R, Khanfir H (2018) Hydrogeological and hydrochemical investigation of groundwater using environmental isotopes (O-18, H-2, H-3, C-14) and chemical tracers: a case study of the intermediate aquifer, Sfax, southeastern Tunisia. Hydrogeol J 26(4):983–1007

Barzegar R, Moghaddam AA, Nazemi AH, Adamowski J (2018) Evidence for the occurrence of hydrogeochemical processes in the groundwater of Khoy plain, northwestern Iran, using ionic ratios and geochemical modeling. Environ Earth Sci 77(16):597

Bawoke GT, Anteneh ZL, Kehali AT, Mohammedyasin MS, Wudie G (2019) Hydrogeochemical and isotopic signatures of groundwater in the Andasa watershed, Upper Blue Nile basin. Northwest Ethiopia J Afr Earth Sci 160:103617

Belkhiri L, Boudoukha A, Mouni L, Baouz T (2010) Application of multivariate statistical methods and inverse geochemical modeling for characterization of groundwater—a case study: Ain Azel plain (Algeria). Geoderma 159(3–4):390–398

Carucci V, Petitta M, Aravena R (2012) Interaction between shallow and deep aquifers in the Tivoli Plain (Central Italy) enhanced by groundwater extraction: a multi-isotope approach and geochemical modeling. Appl Geochem 27(1):266–280

Chen L, Wan L, Zhang FW, Ma LN, Geng XX (2015a) Characteristics of hydraulic connection between aquifer groups in Jiaozuo mine area. South-to-North Water Transf Water Sci Technol 13(2):330–333 **(in Chinese)**

Chen LZ, Ma T, Ma J, Du Y, Xiao C (2015b) Identification of material source for the salt lakes in the Qaidam Basin. Hydrogeol Eng Geol 42(4):101–107 **(in Chinese)**

Chen LW, Xu DQ, Liu YX, Li SJ, Zhang KX, Yin XX (2017) Study on hydrogeochemical simulation of main inrush aquifers in the Suxian mining area. J Anhui Univ Sci Technol (Nat Sci) 37(6):27–33 **(in Chinese)**

Cortes JE, Munoz LF, Gonzalez CA, Nino JE, Polo A, Suspes A, Siachoque SC, Hernandez A, Trujillo H (2016) Hydrogeochemistry of the formation waters in the San Francisco field, UMV

basin, Colombia—a multivariate statistical approach. J Hydrol 539:113–124
Fu CC, Li XQ, Ma JF, Liu LX, Gao M, Bai ZX (2018) A hydrochemistry and multi-isotopic study of groundwater origin and hydrochemical evolution in the middle reaches of the Kuye River basin. Appl Geochem 98:82–93
Gastmans D, Chang HK, Hutcheon I (2010) Groundwater geochemical evolution in the northern portion of the guarani aquifer system (Brazil) and its relationship to diagenetic features. Appl Geochem 25(1):16–33
Gibbs RJ (1970) Mechanisms controlling world water chemistry. Science 170(3962):1088–1090
He KQ, Guo L, Guo YY, Luo HL, Liang YP (2019) Research on the effects of coal mining on the karst hydrogeological environment in Jiaozuo mining area. China Environ Earth Sci 78:434
Huang PH, Chen JS (2012) Recharge sources and hydrogeochemical evolution of groundwater in the coal-mining district of Jiaozuo. China Hydrogeol J 20(4):739–754
Huang PH, Wang XY (2018a) Piper-PCA-Fisher recognition model of water inrush source: a case study of the Jiaozuo mining area. Geofluids 2018:1–10
Huang PH, Wang XY (2018b) Groundwater-mixing mechanism in a multiaquifer system based on isotopic tracing theory: a case study in a coal mine district, China. Geofluids 2018:1–10
Hussein MT (2004) Hydrochemical evaluation of groundwater in the Blue Nile Basin, eastern Sudan, using conventional and multivariate techniques. Hydrogeol J 12(2):144–158
Ibrahim RGM, Korany EA, Tempel RN, Gomaa MA (2019) Processes of water rock interactions and their impacts upon the groundwater composition in Assiut area, Egypt: Applications of hydrogeochemical and multivariate analysis. J Afr Earth Sci 149:72–83
Jia ZX, Zang HF, Hobbs P, Zheng XQ, Xu YX, Wang K (2017) Application of inverse modeling in a study of the hydrogeochemical evolution of karst groundwater in the Jinci Spring region, northern China. Environ Earth Sci 76(8):312
Jin DW (2002) Research status and outlook of water ourburst from seam floor in China coal mines. Coal Sci Technol 6:1–4 **(in Chinese)**
Jin K, Rao WB, Tan HB, Song YX, Yong B, Zheng FW, Chen TQ, Han LF (2018) H-O isotopic and chemical characteristics of a precipitation-lake water-groundwater system in a desert area. J Hydrol 559:848–860
Li PY (2018) Mine water problems and solutions in China. Mine Water Environ 37:217–221
Li PY, Qian H, Wu JH, Zhang YQ, Zhang HB (2013) Major ion chemistry of shallow groundwater in the Dongsheng coalfield, Ordos basin. China Mine Water Environ 32(3):195–206
Li PY, Tian R, Liu R (2019) Solute geochemistry and multivariate analysis of water quality in the guohua phosphorite mine, Guizhou province. China Expo Health 11(2):81–94
Li PY, Wu JH, Qian H (2016a) Preliminary assessment of hydraulic connectivity between river water and shallow groundwater and estimation of their transfer rate during dry season in the Shidi River. China Environ Earth Sci 75(2):99
Li PY, Wu JH, Qian H (2016b) Hydrochemical appraisal of groundwater quality for drinking and irrigation purposes and the major influencing factors: a case study in and around Hua County. China Arab J Geosci 9(1):15
Li PY, Wu JH, Tian R, He S, He XD, Xue CY, Zhang K (2018) Geochemistry, hydraulic connectivity and quality appraisal of multilayered groundwater in the Hongdunzi coal mine, northwest China. Mine Water Environ 37(2):222–237
Liu F, Song XF, Yang LH, Han DM, Zhang YH, Ma Y, Bu HM (2015) The role of anthropogenic and natural factors in shaping the geochemical evolution of groundwater in the Subei Lake basin, Ordos energy base, Northwestern China. Sci Total Environ 538:327–340
Liu P, Hoth N, Drebenstedt C, Sun YJ, Xu ZM (2017) Hydrogeochemical paths of multi-layer groundwater system in coal mining regions—using multivariate statistics and geochemical modeling approaches. Sci Total Environ 601:1–14
Lopes-Mazzetto JM, Schellekens J, Vidal-Torrado P, Buurman P (2018) Impact of drainage and soil hydrology on sources and degradation of organic matter in tropical coastal podzols. Geoderma 330:79–90
Makni J, Bouri S, Ben Dhia H (2013) Hydrochemistry and geothermometry of thermal groundwater of southeastern Tunisia (Gabes region). Arab J Geosci 6(7):2673–2683
Martinez JL, Raiber M, Cendon DI (2017) Using 3D geological modelling and geochemical mixing models to characterise alluvial aquifer recharge sources in the upper Condamine River catchment, Queensland, Australia. Sci Total Environ 574:1–18
Mendoza OT, Ruiz J, Villasenor ED, Guzman AR, Cortes A, Souto SAS, Almazan AD, Bustos RR (2016) Water-rock-tailings interactions and sources of sulfur and metals in the subtropical mining region of Taxco, Guerrero (southern Mexico): a multi-isotopic approach. Appl Geochem 66:73–81
Moran-Ramirez J, Ledesma-Ruiz R, Mahlknecht J, Ramos-Leal JA (2016) Rock-water interactions and pollution processes in the volcanic aquifer system of Guadalajara, Mexico, using inverse geochemical modeling. Appl Geochem 68:79–94
Peng TR, Huang CC, Wang CH, Liu TK, Lu WC, Chen KY (2012) Using oxygen, hydrogen, and tritium isotopes to assess pond water's contribution to groundwater and local precipitation in the pediment tableland areas of northwestern Taiwan. J Hydrol 450:105–116
Pina A, Donado LD, Blake S, Cramer T (2018) Compositional multivariate statistical analysis of the hydrogeochemical processes in a fractured massif: La Linea tunnel project, Colombia. Appl Geochem 95:1–18
Qi HH, Ma CM, He ZK, Hu XJ, Gao L (2019) Lithium and its isotopes as tracers of groundwater salinization: a study in the southern coastal plain of Laizhou Bay, China. Sci Total Environ 650:878–890
Qian H, Li PY, Wu JH, Zhou YH (2013) Isotopic characteristics of precipitation, surface and ground waters in the Yinchuan plain. Northwest China Environ Earth Sci 70(1):57–70
Qian H, Wu JH, Zhou YH, Li PY (2014) Stable oxygen and hydrogen isotopes as indicators of lake water recharge and evaporation in the lakes of the Yinchuan Plain. Hydrol Process 28(10):3554–3562
Qian JZ, Wang L, Ma L, Lu YH, Zhao WD, Zhang Y (2016) Multivariate statistical analysis of water chemistry in evaluating groundwater geochemical evolution and aquifer connectivity near a large coal mine, Anhui. China Environ Earth Sci 75(9):747
Qiao W (2011) Study on the water abundance regularity for deep fracture-karst aquifer and the critical evaluation of water inrush from coal floor in coal-mine. China Univ of Mining and Technology (in Chinese), PhD Diss
Sako A, Bamba O, Gordio A (2016) Hydrogeochemical processes controlling groundwater quality around Bombore gold mineralized zone, central Burkina Faso. J Geochem Explor 170:58–71
Shi LQ, Qu XY, Han J, Qiu M, Gao WF, Qin DX, Liu HS (2019) Multi-model fusion for assessing the risk of inrush of limestone karst water through mine floor. J China Coal Soc 44(8):2484–2493 **(in Chinese)**
Szymkiewicz A, Gumula-Kawecka A, Simunek J, Leterme B, Beegum S, Jaworrska-Szulc B, Pruszkowska-Caceres M, Gorczewska-Langner W, Angulo-Jaramillo R, Jacques D (2018) Simulations of freshwater lens recharge and salt/freshwater interfaces using the HYDRUS and SWI2 packages for MODFLOW. J Hydrol Hydromech 66(2):246–256

Tizro AT, Voudouris KS (2008) Groundwater quality in the semi-arid region of the Chahardouly basin. West Iran Hydrol Processes 22(16):3066–3078

Voutsis N, Kelepertzis E, Tziritis E, Kelepertsis A (2015) Assessing the hydrogeochemistry of groundwaters in ophiolite areas of Euboea Island, Greece, using multivariate statistical methods. J Geochem Explor 159:79–92

Wang Y, Jiao JJ (2012) Origin of groundwater salinity and hydrogeochemical processes in the confined Quaternary aquifer of the Pearl River Delta, China. J Hydro 438:112–124

Wen TX, Kong XB (2020) Mine water inrush source identification model based on KPCA-PSO-RBF-SVM. J Liaoning Tech Univ (Nat Sci) 39(1):6–11 **(in Chinese)**

Wu JH, Li PY, Qian H, Duan Z, Zhang XD (2014) Using correlation and multivariate statistical analysis to identify hydrogeochemical processes affecting the major ion chemistry of waters: a case study in Laoheba phosphorite mine in Sichuan. China Arab J Geosci 7(10):3973–3982

Wu JH, Li PY, Wang D, Ren XF, Wei MJ (2019) Statistical and multivariate statistical techniques to trace the sources and affecting factors of groundwater pollution in a rapidly growing city on the Chinese Loess Plateau. Hum Ecol Risk Assess 26:1603–1621

Xu K, Dai GL, Duan Z, Xue XY (2018) Hydrogeochemical evolution of an Ordovician limestone aquifer influenced by coal mining: a case study in the Hancheng mining area. China Mine Water Environ 37(2):238–248

Xu PP, Li MN, Qian H, Zhang QY, Liu FX, Hou K (2019) Hydrochemistry and geothermometry of geothermal water in the central Guanzhong Basin, China: a case study in Xi'an. Environ Earth Sci 78(3):87

Yang N, Wang GC, Shi ZM, Zhao D, Jiang WJ, Guo L, Liao F, Zhou PP (2018) Application of multiple approaches to investigate the hydrochemistry evolution of groundwater in an arid region: Nomhon, northwestern China. Water 10(11):1667

Yu SB, Ma ZM, Zhang HS (2012) Pollutant characteristics of shallow groundwater in Jiaozuo site of the middle south-to-north water diversion project. J Univ Jinan 26(1):91–95 **(in Chinese)**

Zhang D, Liu CQ, Yin GX (2010) Study on inland groundwater salinization based on stable isotope and hydrochemistry :a case study in Jiaozuo city. China Earth Environ 38(2):177–183 **(in Chinese)**

Zhang XD, Qian H, Chen J, Qiao L (2014) Assessment of groundwater chemistry and status in a heavily used semi-arid region with multivariate statistical analysis. Water 6(8):2212–2232

Zhang H, Xing HF, Yao DX, Liu LL, Xue DR, Guo F (2019a) The multiple logistic regression recognition model for mine water inrush source based on cluster analysis. Environ Earth Sci 78(20):612

Zhang Y, Guo CQ, Zhu YG, Yu S (2019b) Chemical characteristics of groundwater and material sources analysis in Buckwheat field. Yunnan Province Environ Sci 40(6):2686–2695 **(in Chinese)**

Zhao SN (2017) The research of temporal and spatial distribution of SO_4^{2-} pollution in the shallow groundwater between two drainage rivers, MSc thesis, Henan Polytech Univ**(in Chinese)**